Dance of the Dragonfly: A Vision-based Agile Aerial Touch Solution for IARC Mission 7

Ziliang Lai, Rui Yang, Hui Cheng*, Wenjun Deng, Kan Wu, and Jianjin Xiao

Abstract— The International Aerial Robotics Competition (IARC) aims to move the state-of-the-art in aerial robotics forward through mission challenges. In the IARC Mission 7, the aerial robot will navigate without external navigation aids, interact with autonomous ground robots, and avoid dynamic obstacles in the herding problem. In 2017 competition, our team firstly accomplished to interactively herd one iRobot to one end of the arena through accurate and rapid aerial touch and won the first place in system control. This paper presents the self-localization, control and tracking strategies for a micro unmanned aerial vehicle (UAV) to accurately and agilely touch ground moving robots. A real-time self-localization framework is proposed to estimate the ego motion of the UAV. A computationally efficient visual tracking scheme is designed to detect the ground robot and estimate its direction. Inspired by the dance of the dragonfly, tracking and control schemes are presented for the UAV to achieve 3-D agile interaction with ground autonomous robots. Simulation and flight experimental results validate the effectiveness of the proposed methods.

I. INTRODUCTION

The International Aerial Robotics Competition (IARC) aims to move the state-of-the-art in aerial robotics forward through the creation of significant and useful mission challenges. In addition to develop solutions for full autonomy and obstacle avoidance, the IARC Mission 7 took a monumental leap by requiring autonomous aerial robots to interact with and control autonomous ground robots [1]. In Mission 7 challenge, teams were tasked with developing systems to locate and herd at least four iRobots toward one end of the arena in less than 10 minutes. The UAV will autonomously interact with the iRobots by top-touch or interception while avoid the dynamic obstacles. J. L. Sanchez-Lopez etc. [2] presented their hardware and software solutions to the Mission 7 challenge, and the visual localization and mapping algorithm, the control algorithms, the mission planner and the safety measures are addressed. Although the Mission 7 has not been accomplished by any team since 2014 due to difficult challenges, some major sub-tasks have been fulfilled. In 2017 competition, our team firstly accomplished to interactively herd one iRobot to one end of the arena through accurate and rapid aerial touch. In this paper, we present the self-localization, control and tracking strategies for an UAV to perform agilely aerial touch on ground autonomous robots.

Related Work

The authors are with Sun Yat-sen University, Guangzhou, China.
*Corresponding author: chengh9@mail.sysu.edu.cn

Fig. 1: Dance of the dragonfly: Dragonflies touch the surface of water to lay eggs on marshy weeds.

Micro UAVs have received growing research interests on full state estimation, autonomous navigation, visual tracking and aerial manipulation [3][4][5] for their wide applications in rescue and surveillance, aerial observation, transportation, etc [6][7]. Interaction between the aerial robots with environments is crucial in aerial manipulation tasks such as touching, grasping and placing objects. In dynamic aerial manipulation tasks, real-time detection of the moving target as well as quick tracking control are critical to achieve agile maneuvering for the UAVs. Self-localization is also important when the UAVs autonomously navigate in GPS-denied environments. Moreover, vision-based aerial manipulation are challenging for micro UAVs due to the limited onboard sensing and computational capabilities. To overcome these problems, many research efforts have been devoted to stability analysis, control laws, visual servoing schemes and mechanism design to perform aerial manipulation tasks. In [8], a model and control methodology is presented to perform mobile manipulating UAV, and the interactions with the environment during the manipulation are studied. Inspired by aerial hunting by birds of prey, a quadrotor equipped with an actuated appendage is designed to enable grasping at high speeds [9]. Following the research [9], a visual servoing scheme is presented in [10] for micro UAV to perform aerial grasping a static cylinder. In [11], a passive mechanism is designed to enable a rotorcraft to passively perch on multiple surfaces.

Vision-based tracking of moving targets for UAVs is demanding in a wide range of applications [3][12]. In [13], visual tracking scenarios of autonomous helicopters have been investigated via simulations. Several visual algorithms to track the predefined targets have been implemented on UAVs [14][15], where simple trackers such as the color and shape filtering are used for specific target tracking. In [16], to achieve stable and robust tracking maneuvering target,
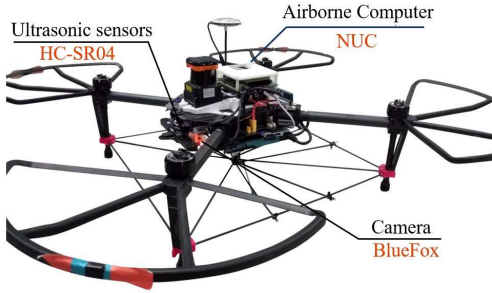
Fig. 2: The developed DJI M100 Platform with onboard sensors and a NUC computer.

vision-based tracking of UAVs is systematically studied considering both visual trackers and the control laws. In [17], a vision-based approach is proposed for a UAV autonomously tracking and landing on a ground moving vehicle.

Different from previous work focusing on aerial manipulating static objects or visual tracking, the paper proposes a vision-based interaction strategy to perform agile aerial touch tasks on moving targets in GPS-denied environments. The primary contribution of the paper is to enable stable and rapid aerial touching the ground moving robots for UAVs using onboard sensing and computation.

The rest of the paper is organized as follows. In Section II, the system architecture is described. Section III designs a self-localization framework via data fusing. Visual detection, control and tracking strategies are proposed in Section IV. Section V presents simulation and experimental results. Conclusions and future work are discussed in Section VI.

II. SYSTEM STRUCTURE

A DJI Matrix 100 shown in Fig. 2 is used as the UAV platform, which is equipped with an onboard BlueFox camera and an Intel NUC core i5 mini PC. BlueFox camera is used to provide image data for both optical flow and target detection. The attitude is estimated by fusing measurements of IMU, and the altitude is measured by an ultrasonic sensor.

The system architecture is shown in Fig. 3. The self-localization scheme estimates the ego motion of the UAV. The visual tracking algorithm detects the moving target and estimates its direction, which is feedback to the high-level controller. The frequency of the video stream and the control signal is 50Hz. The UAV communicates with the ground station via Wi-Fi, through which the flight can be monitored and algorithm parameters can be adjusted conveniently. Remote control is utilized to pull the UAV back in an emergency.

III. SELF-LOCALIZATION STRATEGY

Reliable and accurate self-localization of UAVs is crucial for full autonomy in GPS-denied environments. In this section, a real-time and computationally efficient framework is proposed to estimate the ego motion of the UAV using commercial and light-weight onboard sensors.
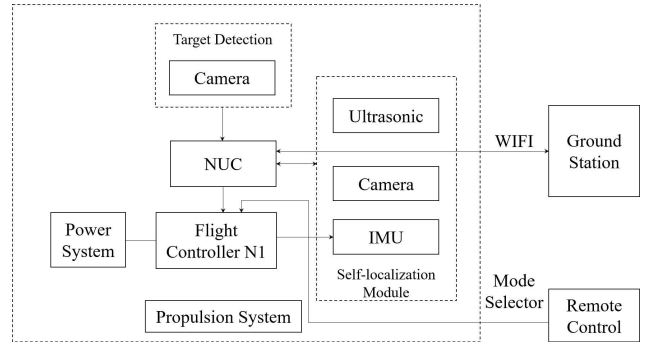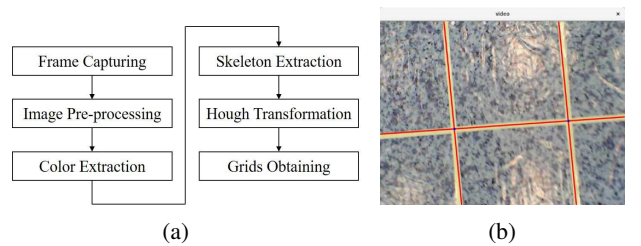

Fig. 3: System architecture of the micro UAV.

Fig. 4: Grid pattern recognition. (a) extract grids; (b) recognition result.

A. Optical flow based Odometry

The LK method [18] is applied to compute optical flow, while a feature selection scheme [19] is used to mitigate the noise effects. The pixel-scale optical flow $[\dot{u}, \dot{v}]^T$ is then converted to the horizontal velocity of the UAV by integrating angular velocity and altitude. Using the pinhole camera model, the horizontal velocity $[T_x, T_y]^T$ can be computed as:

$$
\begin{aligned}
T_x &= \frac{\dot{u}z_c}{f} - \omega_y z_c \\
T_y &= \frac{\dot{v}z_c}{f} + \omega_x z_c \\
z_c &= \frac{h}{\cos\theta\cos\phi}
\end{aligned}
\tag{1}
$$

where w_x/w_y denote roll/pitch angular velocities, respectively, f is the focal length of camera, and z_c is the distant from camera to the tracking feature on the ground estimated by altitude h.

B. Grid Pattern Positioning

In order to mitigate accumulative error of the optical flow based odometry, information of the structural grid arena can be used in IARC Mission 7. As shown in Fig. 4, the grids are extracted from the video, then the extracted grids are projected into the arena frame and matched with the corresponding grids in the arena. The relative position of the UAV to the grid points, Δp, is estimated by:

$$
\Delta p = \left[\frac{uz}{f},\ \frac{vz}{f},\ z\right]^T
\tag{2}
$$

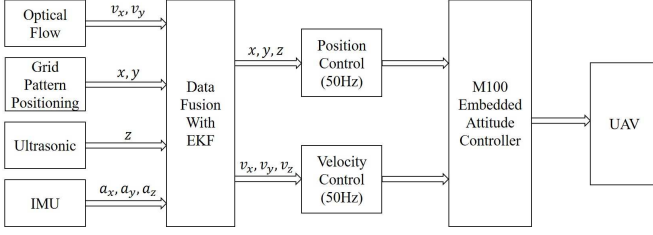where $[u, v]^T$ denotes the position of grid point in the image

Fig. 5: Self-localization of the UAV using EKF based data fusion.

Fig. 6: Real-time moving robot detection and tracking.

plane, f is the focal length of camera, and z is the vertical distance to the grid point in body frame. z can be computed as:

$$z = \frac{h}{-\frac{u}{f}\sin\theta + \frac{v}{f}\sin\phi\cos\theta + \cos\phi\cos\theta} \quad (3)$$

where h denotes the altitude. θ and ϕ denote the pitch and roll angles, respectively.

C. Data Fusion based Self-Localization

To achieve robust and accurate state estimation for the UAV using onboard sensors, the extended Kalman filter (EKF) is employed to fuse the estimated states from the optical flow based odometry, grid pattern positioning, ultrasonic and IMU. The framework of the data fusion based self-localization scheme is illustrated in Fig.5.

To estimate the full states $\boldsymbol{x} = [x, y, z, v_x, v_y, v_z]^T$ of the UAV in global coordinates, the linearly approximate dynamic model and the measurement model are given as:

$$\begin{aligned} \boldsymbol{x}_t &= \boldsymbol{A}\boldsymbol{x}_{t-1}\boldsymbol{B}\boldsymbol{a}_t + \boldsymbol{w}_t \\ \boldsymbol{z}_t &= \boldsymbol{H}\boldsymbol{x}_t + \boldsymbol{v}_t \end{aligned} \quad (4)$$

where $\boldsymbol{w}_t$ and $\boldsymbol{v}_t$ are Gaussian noise, $\boldsymbol{a}_t$ denotes the acceleration measured by IMU, and matrices $\boldsymbol{A}$ and $\boldsymbol{B}$ are given by:

$$\boldsymbol{A} = \begin{bmatrix} 1 & 0 & 0 & \Delta t & 0 & 0 \\ 0 & 1 & 0 & 0 & \Delta t & 0 \\ 0 & 0 & 1 & 0 & 0 & \Delta t \\ 0 & 0 & 0 & 1 & 0 & 0 \\ 0 & 0 & 0 & 0 & 1 & 0 \\ 0 & 0 & 0 & 0 & 0 & 1 \end{bmatrix}$$

$$\boldsymbol{B} = \begin{bmatrix} \frac{1}{2}\Delta t^2 & 0 & 0 \\ 0 & \frac{1}{2}\Delta t^2 & 0 \\ 0 & 0 & \frac{1}{2}\Delta t^2 \\ \Delta t & 0 & 0 \\ 0 & \Delta t & 0 \\ 0 & 0 & \Delta t \end{bmatrix}$$

$\boldsymbol{H}$ has different values for different sensors or targets. For instance, in the optical flow based odometry,

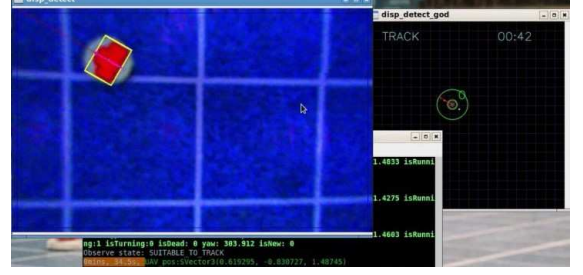$$\boldsymbol{H} = \begin{bmatrix} 0 & 0 & 0 & 1 & 0 & 0 \\ 0 & 0 & 0 & 0 & 1 & 0 \end{bmatrix}$$

The system states are iteratively estimated using the Kalman filter:

$$\begin{aligned} \bar{\boldsymbol{x}}_t &= \boldsymbol{A}\boldsymbol{x}_{t-1} + \boldsymbol{B}\boldsymbol{u}_t \\ \bar{\boldsymbol{\Sigma}}_t &= \boldsymbol{A}\boldsymbol{\Sigma}_{t-1}\boldsymbol{A}^T + \boldsymbol{R}_t \\ \boldsymbol{K}_t &= \bar{\boldsymbol{\Sigma}}_t\boldsymbol{H}^T\left(\boldsymbol{H}\bar{\boldsymbol{\Sigma}}_t\boldsymbol{H}^T + \boldsymbol{Q}_t\right)^{-1} \\ \boldsymbol{x}_t &= \bar{\boldsymbol{x}}_t + \boldsymbol{K}_t\left(\boldsymbol{z}_t - \boldsymbol{H}\bar{\boldsymbol{x}}_t\right) \\ \boldsymbol{\Sigma}_t &= \left(\boldsymbol{I} - \boldsymbol{K}_t\boldsymbol{H}\right)\bar{\boldsymbol{\Sigma}}_t \end{aligned} \quad (5)$$

where $\boldsymbol{R}_t$ and $\boldsymbol{Q}_t$ are covariance of $\boldsymbol{w}_t$ and $\boldsymbol{v}_t$.

IV. AERIAL TOUCHING GROUND AUTONOMOUS ROBOTS

In this section, a computationally efficient visual tracking scheme is firstly presented to detect the ground robot and estimate its direction. Inspired by the dance of the dragonfly, tracking and control schemes are proposed for the UAV to achieve 3-D agile interaction with ground robots.

A. Detection of Ground Autonomous Robots

A robust visual detection scheme is presented to detect and track the ground robots, and its direction is estimated using distinguishable color and shape, as shown in Fig. 6.

Firstly, regions of interest are selected by color. A 3-D table indexed by RGB color components is pre-constructed and checking whether a pixel is desired or not is simply looking up the corresponding entry indexed by the color. Since the desired color region can be manually constructed and adjusted in the table, it is much more robust than threshold or classifier approaches. Secondly, shape information is considered to extract regions of targets from other noise blocks. Shape of each region is represented by its contour. Metrics of the contour including moments, area and perimeter are utilized as evidences for targets. If all metrics are within the expected range, the region is estimated as a target robot.

The KCF algorithm [20] is utilized to track the moving target robot. The special shape is also used to determine the moving direction of the robot, while its speed is assumed to be constant. The relative position between the UAV and the ground robot can be estimated by (2). Using the 6-D state estimation of the UAV, the position of the ground robot in the arena can be obtained.
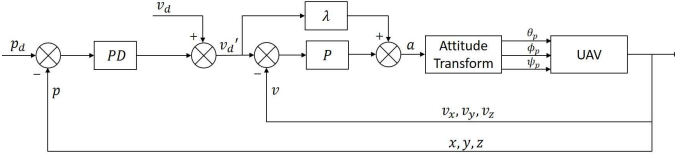
Fig. 7: A cascaded PID controller for position control.

Fig. 8: Tracking control configuration of the UAV.

Fig. 9: The target is moving towards the UAV.

B. Position Control of the UAV

The DJI N1 flight controller provide API to drive the M100 platform to perform hovering, landing or trajectory tracking with satisfied control performance in normal applications. However, the control system of the DJI N1 is fixed and not flexible for some customized applications. The landing of the DJI N1 API is slow for safety operation and not feasible for quick interaction tasks. In this section, we design a position controller for the UAV to achieve rapid 3-D aerial touch using the full states estimation, while use the DJI N1 API to control the attitude and throttle.

1) Cascaded PID for Position Control: For the M100 platform, the force U_1 produced by four motors can be set via the throttle input interface. Assume that U_1 is linear with the throttle parameter T, that is, $U_1 = -cT$, in which c is a ratio coefficient, $T > 0$. The attitude and throttle of the UAV can be calculated as [6].

$$
\begin{cases}
\theta = -\dfrac{1}{cT}\left(\ddot{X}\cos\psi + \ddot{Y}\sin\psi\right) \\[2mm]
\phi = -\dfrac{1}{cT}\left(\ddot{X}\sin\psi - \ddot{Y}\cos\psi\right) \\[2mm]
T = -\dfrac{\ddot{Z} - g}{c \cdot \cos\phi \cos\theta}
\end{cases}
\tag{6}
$$

where X, Y and Z are the global coordinates of the UAV.

A cascaded PID controller involving feedback and feed-forward control is illustrated in Fig. 7. The expected position $\boldsymbol{p_d}$ is input to the controller, while the estimated position $\boldsymbol{p}$ and velocity $\boldsymbol{v}$ of the UAV are served as feedback signals. The computed value of the velocity control loop is feed-forwarded as the expected acceleration $\boldsymbol{a}$. The computed throttle and expected attitude are used as the input of the attitude controller after attitude transform.

The control law of the position loop is formulated as follows:

$$
\begin{aligned}
\boldsymbol{e}_p &= \boldsymbol{p}_d - \boldsymbol{p} \\
\boldsymbol{u}_p &= \boldsymbol{k}_p \boldsymbol{e}_p + \boldsymbol{k}_d \dot{\boldsymbol{p}}
\end{aligned}
\tag{7}
$$

where $\boldsymbol{p}_d = [\boldsymbol{x}_d, \boldsymbol{y}_d, \boldsymbol{z}_d]^T$ denotes the expected position of UAV in the world frame, and $\boldsymbol{k}_p = [k_{px}, k_{py}, k_{pz}]^T$ and $\boldsymbol{k}_d = [k_{dx}, k_{dy}, k_{dz}]^T$ are the proportional and differential coefficients, respectively.

The control law of velocity loop is formulated as follows:

$$
\begin{aligned}
\boldsymbol{e}_v &= \boldsymbol{v}'_d - \boldsymbol{v} \\
\boldsymbol{u}_v &= \boldsymbol{k}_v \boldsymbol{e}_v + \boldsymbol{\lambda}\boldsymbol{v}'_d
\end{aligned}
\tag{8}
$$

where $\boldsymbol{v}'_d = \boldsymbol{v}_d + \boldsymbol{u}_p$ is the velocity set point derived from the position loop, and $\boldsymbol{k}_v = [k_{vx}, k_{vy}, k_{vz}]^T$ are the proportional coefficients.
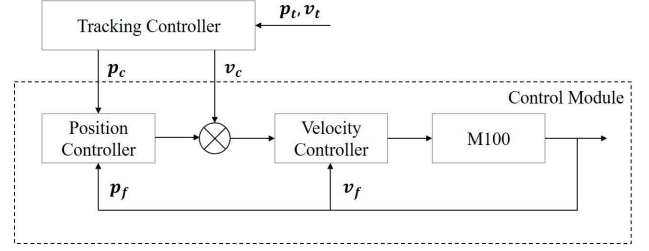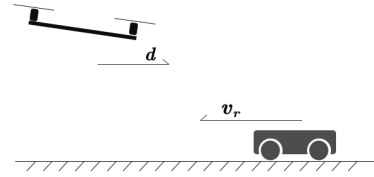
2) Adaptive parameter Adjustment: In applications, power consumption of the UAV is large when keeping rapid and continuous flight. The dynamic parameters of the system will vary unpredictably, leading to difficulties in tuning the controllers. An adaptive parameter adjustment method is proposed to solve this problem. Assume that the throttle parameter in the attitude controller is approximately linear with the acceleration produced by the motors. With the assumption, define the parameter c as the ratio of the force to the throttle. The time-varying parameter c can be adaptively updated according to:

$$
c_n = c_{n-1}\alpha + \frac{g}{T}\left(1 - \alpha\right)
\tag{9}
$$

where c_n is the updated value from c_{n-1} in the n iteration phase, α is the filter parameter.

C. Aerial Tracking and Touching

In this section, control laws for the UAV to perform smooth tracking and rapid touching are presented. Denote $\boldsymbol{p_t}$ and $\boldsymbol{v_t}$ as the estimated position and velocity of the moving target. The tracking control configuration is shown in Fig. 8.

To track position of the target, the position tracking controller is given as:

$$
\boldsymbol{p}_c = \boldsymbol{p}_t
\tag{10}
$$

A natural way for velocity tracking is to set $\boldsymbol{v}_c$ is to set $\boldsymbol{v}_c = \boldsymbol{v}_r$. However, when the target is moving to the UAV as illustrated in Fig. 9, the output of position controller is cancelled with the designated $\boldsymbol{v}_c$, causing slow approaching.

To cope with such situations, a simple and efficient velocity control law is given as:

$$
\boldsymbol{v}_c = \begin{cases} \boldsymbol{v}_r & \boldsymbol{d} \cdot \boldsymbol{v}_r > 0 \\ \boldsymbol{v}_r \exp\left(-|\boldsymbol{d}|\right) & \boldsymbol{d} \cdot \boldsymbol{v}_r < 0 \end{cases}
\tag{11}
$$

where d denotes the vector directing from the UAV to the target.

Tracking involves horizontal control. In 3-D aerial touch tasks, vertical control laws should be developed to achieve quick diving and arising. The aerial touch action is designed to emulate a dragonfly flying over water. During the aerial touch process, the UAV firstly tracks the ground target and descents to 0.8m above it. After a short time tracking, the UAV quickly dives down, touch the top of ground robot and immediately arise to normal altitude for the next observation and touch.

V. SIMULATION AND EXPERIMENTAL VALIDATION

In this section, simulation and experimental results are presented and discussed to validate the effectiveness of the proposed vision-based aerial touch solution.

A. Simulator

As shown in Fig. 10, a simulator is developed with OpenGL to verify the aerial touch strategy. The simulator can provide a scene from an onboard RGB camera, communicate with the platform using M100 onboard-SDK, and simulate the flight of the UAV. In the simulator, the UAV can stably fly on the arena, detect, track and touch the ground robots based on the proposed strategy.

B. Simulation and Experimental Results

Extensive flight experiments have been performed in indoor and outdoor environments to test and verify the proposed aerial touch strategy using the DJI M100 platform equipped with onboard sensors and mini computers.

The estimated horizontal position of the UAV using optical flow odometry and grid pattern positioning is depicted in Fig. 11. It can be shown that the displacement of the optical flow odometry is compensated by the grid pattern positioning. With the grid compensation, the horizontal displacement of the UAV is within 1cm.

Fig. 12 depicts the localization performance estimated by the proposed data fusion scheme. The UAV was manually shaken back and forth during the experiments. It can be shown from Fig. 12 that the estimated horizontal velocity and displacement after EKF based data fusing is more smooth and robust than the estimate of the optical flow odometry and the grid positioning method.

To illustrate the performance of the proposed vertical position controller, the UAV is instructed to autonomously takeoff with desired altitude of 1.5m. Fig. 13 shows that less overshooting can be achieved using feed-forward control component. In addition, to verify the performance of horizontal position control, the UAV is controlled to follow a rectangle. The flight trajectories of the UAV and the reference rectangle are depicted in Fig. 14. It can be shown from Fig. 14 that the UAV can track the reference rectangle smoothly. The simulation results are also given in Fig. 13 and Fig. 14 to show the consistency of the algorithm in both ideal and real-world environment.

To validate the tracking performance, the UAV autonomously tracks a virtual target running in circular path
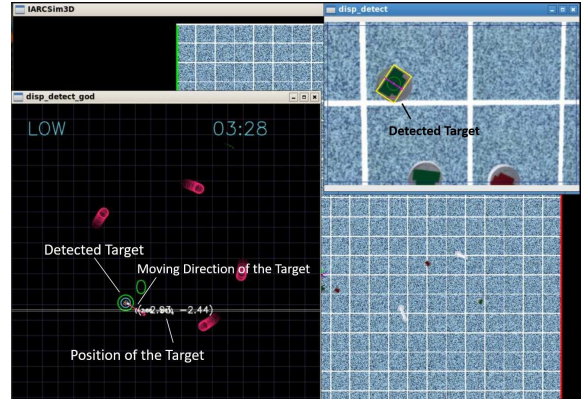

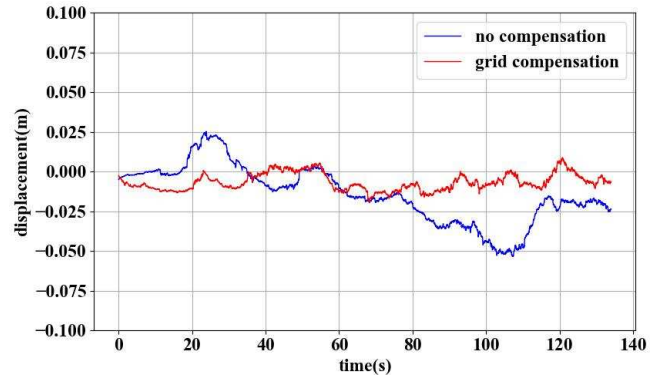Fig. 10: Simulator is developed to verify the aerial touch strategy.

Fig. 11: Estimated displacement of the UAV using optical flow odometry and grid pattern positioning, respectively. The red line is with the compensation of the grid pattern positioning, while the blue line plots the displacement estimated by the optical flow odometry.

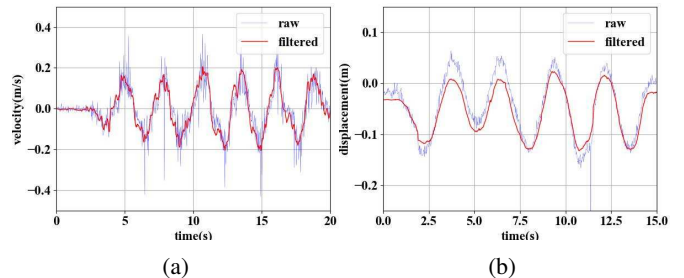
(a)   (b)

Fig. 12: The localization performance estimated by the proposed data fusion scheme. (a) estimated horizontal velocity, where the red line is the velocity estimation of the EKF, while the blue line denotes the estimate by the optical flow; (b) estimated horizontal displacement, where the red line is the estimated displacement of the EKF, while the blue line denotes the estimate by the grid positioning method.
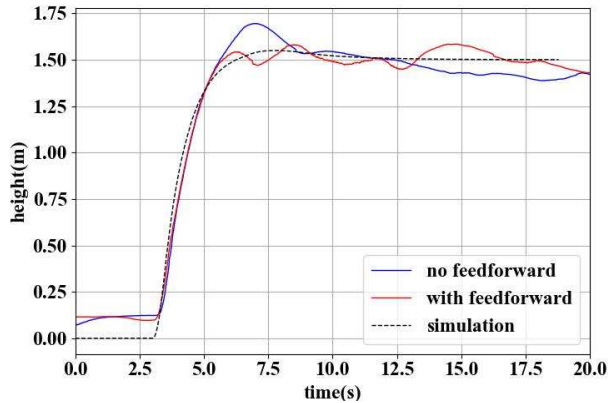
Fig. 13: Vertical control performance, where the blue/red lines are with/without feed-forward component, respectively, in flight experiments. The dashed line depicts the simulation result with feed-forward component.
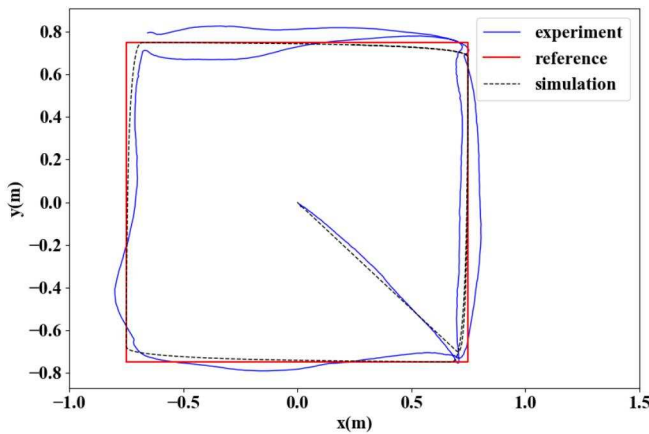

Fig. 14: Horizontal control performance, where the red line is the reference path, while the dashed black/blue lines are the flight paths of the UAV in simulation and flight experiment, respectively.
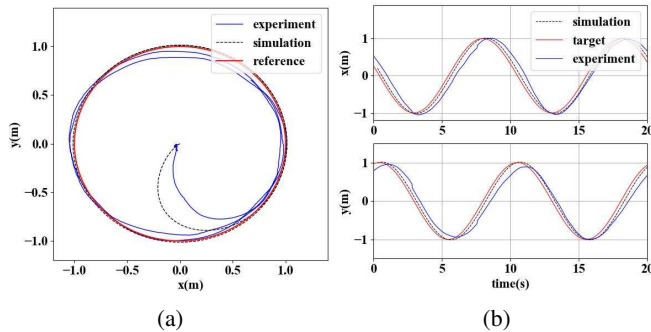

Fig. 15: Trajectory tracking on a virtual target running in circular path with radius of 1m, where the red path is the reference circle, and the dashed black/blue paths are the flight trajectories of the UAV in simulation and flight experiments, respectively. (a) flight trajectories in the aspect of x and y; (b) flight trajectories with respect to time.
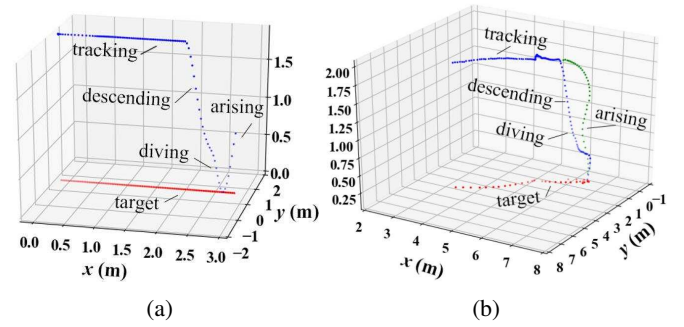

Fig. 16: The 3-D flight trajectory of the UAV during the aerial touch process. (a) simulation result; (b) flight experimental result.

Fig. 17: Snap shots of the UAV during the aerial touch process.

with radius of 1m. The UAV takes off in the center of the circle which is far away from the target. The blue lines shown in Fig. 15 illustrate that the UAV can track a ground moving target accurately. It is noted that the UAV acquires smooth tracking performance.

To illustrate the aerial touch process, 3-D flight trajectories in simulation and experiment are depicted in Fig. 16 (a) and (b), respectively. The UAV first tracks the ground moving robot, then performs diving and rapidly touch the top of the ground robot. After the aerial touch action, the UAV arises immediately. In the arising phase, the UAV still tracks the target and prepares for the next touch. The trajectory of the touching process in experiment is slightly different from the ideal one in simulation because of the pose recovering after touching. Fig. 17 illustrated the snap shots of the UAV during the aerial touch process.

A demo video can be found online at [21].

VI. CONCLUSION

This paper presents a vision-based aerial touch solution for UAVs in GPS-denied environments. A real-time self-localization strategy using EKF is proposed to provide robust and accurate localization estimate. Using the estimated 6-D states of the UAV, a cascaded PID controller with adaptive parameter adjustment is designed to provide fast and stable position control. A computationally efficient detection scheme is presented to detect the ground target robot and estimate its moving direction. Tracking and touching control schemes are proposed to perform agile 3-D aerial touch on ground autonomous robots. Simulation and experimental results illustrate that the proposed aerial touch solution can achieve smooth tracking and quick touch accurately and

stably. In the future work, the design of the manipulating mechanism will be considered, and aerial grasping will be studied using onboard monocular vision. Moreover, the cooperative transportation of the UAVs will be investigated.

Acknowledgement

REFERENCES

[1] http://www.aerialroboticscompetition.org/index.php.

[2] J. L. Sanchez-Lopez, J. Pestana, J. F. Collumeau, etc., A Vision Based Aerial Robot solution for the Mission 7 of the International Aerial Robotics Competition, Prof. of International Conference on Unmanned Aircraft Systems (ICUAS), pp. 1391-1400, Denver, Colorado, USA, June 2015.

[3] C. Teuliere, L. Eck, and E. Marchand, Chasing a moving target from a flying uav, Proc. of IEEE/RSJ Int. Conf. on in Intelligent Robots and Systems (IROS), pp. 4929-4934, San Francisco, California, USA, Sept. 2011.

[4] A. Bry, A. Bachrach and N. Roy, State estimation for aggressive flight in GPS-denied environments using onboard sensing, Proc. of IEEE Conf. Robotics and Automation, pp. 1-8, Minnesota, USA, May 2012.

[5] S. Grzonka, G. Grisetti and W. Burgard, A fully autonomous indoor quadrotor, IEEE Trans. Robotics, Vol. 28, pp. 90-100, 2012.

[6] R. Mahony, V. Kumar, and P. Corke, Multirotor aerial vehicles, IEEE Robotics and Automation magazine, vol. 20, no. 32, 2012.

[7] G. Bevacqua, J. Cacace, A. Finzi, and V. Lippiello, Mixed-initiative planning and execution for multiple drones in search and rescue missions, Proc. of Int. Conf. on Automated Planning and Scheduling, pp. 315-323, 2015.

[8] Matko Orsag, Christopher Korpela, Paul Oh, "Modeling and Control of MM-UAV: Mobile Manipulating Unmanned Aerial Vehicle", Journal of Intelligent and Robotic Systems, vol. 69, pp. 1-4, August 2012.

[9] Justin Thomas, Joe Polin, Koushil Sreenath, Vijay Kumar, "Avian-Inspired Grasping for Quadrotor Micro UAVs", Proc. of Int. Design and Engineering Technical Conf.and Computers and Information in Engineering Conf. (IDETC/CIE), Portland, Oregon, USA, August 2013.

[10] Justin Thomas, Giuseppe Loianno, Koushil Sreenath, and Vijay Kumar, Toward image based visual servoing for aerial grasping and perching, Proc. of IEEE Conf. on Robotics and Automation (ICRA), Hong Kong, China, May 2014.

[11] Courtney E. Doyle, Justin J. Bird, Taylor A. Isom, etc, An Avian-Inspired Passive Mechanism for Quadrotor Perching, IEEE/ASME Transactions on Mechatronics, vol. 18, no. 2, pp. 506517, April 2014.

[12] A. G. Kendall, N. N. Salvapantula, and K. A. Stol, On-board object tracking control of a quadcopter with monocular vision, Proc. of IEEE Int. Conf. on Unmanned Aircraft Systems (ICUAS), pp. 404-411, Orlando, FL, USA, May 2014

[13] A. Razinkova and H.-C. Cho, Tracking a moving ground object using quadcopter UAV in a presence of noise, Proc. of IEEE Conf. on Advanced Intelligent Mechatronics, pp. 1546-1551, Busan, Korea, 2015.

[14] F. Lin, X. Dong, B. M. Chen, K.-Y. Lum, and T. H. Lee, A robust real-time embedded vision system on an unmanned rotorcraft for ground target following, IEEE Transactions on Industrial Electronics, vol. 59, no. 2, pp. 1038-1049, 2012.

[15] A. Chakrabarty, R. Morris, X. Bouyssounouse, and R. Hunt, Autonomous indoor object tracking with the Parrot AR. Drone, Proc. of IEEE Int. Conf. on Unmanned Aircraft Systems (ICUAS), pp. 25-30, Washington D.C., USA, June 2016.

[16] H. Cheng, L.S. Lin, Z.Q. Zheng, Y.W. Guan, and Z.C. Liu, An Autonomous Vision-Based Target Tracking System for Rotorcraft Unmanned Aerial Vehicles, Proc. of IEEE/RSJ Int. Conf. on Intelligent Robots and Systems (IROS), pp. 1732-1738, Vancouver, BC, Canada, Sep. 2017.

[17] H. Cheng, Y. S. Chen, X. K. Li and W. S. Wong, Autonomous Hovering, Tracking and Landing of a UAV on a Moving UGV using Onboard Monocular Vision, in Proc. 32nd Chinese Control Conf., pp. 5895-5901, Xian, China, July 2013.

[18] Bruce D. Lucas and Takeo Kanade, An iterative image registration technique with an application to stereo vision, Proc. of Int. Joint Conference on Artificial Intelligence (IJCAI), pp. 674-679, Vancouver, BC, Canada, August 1981.

[19] J. B. Shi and C. Tomasi, Good features to track, Proc. of IEEE Computer Vision and Pattern Recognition, Seattle, pp. 593-600, WA, USA, June 1994.

[20] J. F. Henriques, R. Caseiro, P. Martins, and J. Batista,High-speed tracking with kernelized correlation filters, IEEE Trans. on Pattern Analysis and Machine Intelligence, vol. 37, no. 3, pp. 583-596, 2015.

[21] Demo video online available at: https://youtu.be/Rr98A2be5Fo